Bioactive Materials 7 (2022) 144–153

Contents lists available at ScienceDirect

Bioactive Materials

journal homepage: www.sciencedirect.com/journal/bioactive-materials

A surface-eroding poly(1,3-trimethylene carbonate) coating for magnesium based cardiovascular stents with stable drug release and improved corrosion resistance

Hongyan Tang [a], Shuangshuang Li [a], Yuan Zhao [a], Cunli Liu [a], Xuenan Gu [a,b,*], Yubo Fan [a,b,**]

[a] Key Laboratory for Biomechanics and Mechanobiology of Ministry of Education, School of Biological Science and Medical Engineering, Beihang University, Beijing, 10083, China
[b] Beijing Advanced Innovation Centre for Biomedical Engineering, Beihang University, Beijing, 102402, China

ARTICLE INFO

Keywords:
Magnesium alloy
Polymeric coating
Surface erosion
Drug release
Cardiovascular stents

ABSTRACT

Magnesium alloys with integration of degradability and good mechanical performance are desired for vascular stent application. Drug-eluting coatings may optimize the corrosion profiles of magnesium substrate and reduce the incidence of restenosis simultaneously. In this paper, poly (trimethylene carbonate) (PTMC) with different molecular weight (50,000 g/mol named as PTMC5 and 350,000 g/mol named as PTMC35) was applied as drug-eluting coatings on magnesium alloys. A conventional antiproliferative drug, paclitaxel (PTX), was incorporated in the PTMC coating. The adhesive strength, corrosion behavior, drug release and biocompatibility were investigated. Compared with the PLGA control group, PTMC coating was uniform and gradually degraded from surface to inside, which could provide long-term protection for the magnesium substrate. PTMC35 coated samples exhibited much slower corrosion rate 0.05 μA/cm^2 in comparison with 0.11 μA/cm^2 and 0.13 μA/cm^2 for PLGA and PTMC5 coated counterparts. In addition, PTMC35 coating showed more stable and sustained drug release ability and effectively inhibited the proliferation of human umbilical vein vascular smooth muscle cells. Hemocompatibility test indicated that few platelets were adhered on PTMC5 and PTMC35 coatings. PTMC35 coating, exhibiting surface erosion behavior, stable drug release and good biocompatibility, could be a good candidate as a drug-eluting coating for magnesium-based stent.

1. Introduction

Permanent metal stents are one of the most effective treatment options in cardiovascular interventions. However, concerns have been raised about their permanently presence in blood vessels, such as sustained physical irritation, inability of vascular remodeling, thrombogenicity, disadvantageous characteristics for future imaging or coronary surgical options. Biodegradable stents may overcome these drawbacks, which can provide sufficient but temporary scaffolding of the blood vessels [1,2]. Magnesium and its alloys exhibit appropriate mechanical support and the ability to degrade safely in human body, and thus are promising candidates for biodegradable stent applications [1,3,4].

Unfortunately, the rapid degradation of magnesium alloy and the resulted fast strength decay in the physiological environment can cause the alloy to loss its mechanical integrity prior to optimal vascular remodeling [5,6], which limits its clinical application. Many efforts have been devoted to increase the corrosion resistance of magnesium alloys via surface coating, including metal oxide coatings [7], fluoride coatings [8,9], calcium phosphate coatings [10,11] and polymeric coatings [12,13]. Amongst these options, polymeric coatings are superior to other materials to serve as the stent coatings because of their additional advantages as a drug reservoir and can be further functionalized with biomolecules. Poly (lactic-*co*-glycolic acid) (PLGA), poly (L-lactide) acid (PLLA) and polycaprolactone (PCL) have been extensively used in permanent metal based drug eluting stents [14,15]. Nevertheless, there are some drawbacks when they are applied on the surface of magnesium

Peer review under responsibility of KeAi Communications Co., Ltd.
* Corresponding author. Key Laboratory for Biomechanics and Mechanobiology of Ministry of Education, School of Biological Science and Medical Engineering, Beihang University, Beijing, 10083, China.
** Corresponding author. Beijing Advanced Innovation Centre for Biomedical Engineering, Beihang University, Beijing, 102402, China.
E-mail addresses: xngu@buaa.edu.cn (X. Gu), yubofan@buaa.edu.cn (Y. Fan).

https://doi.org/10.1016/j.bioactmat.2021.05.045
Received 24 October 2020; Received in revised form 13 April 2021; Accepted 26 May 2021
Available online 6 June 2021

alloys. Their acidic degradation products and bulk degradation behavior may undermine rather than enhance the corrosion resistance of magnesium substrate [16]. Moreover, the rapid hydrogen evolution of magnesium alloys usually leads to the formation of gas pockets under the coating, which may cause the delamination of polymer pieces from the stent, resulting in deleterious consequences for clinical use [17].

The objective of this study is to develop degradable polymer coatings which do not produce acidic degradation products and is applicable to the blood-contacting stents. This requirement can be fulfilled by using PTMC, the degradation product of which is completely neutral. Degradation of PTMC is characterized by surface erosion, which may minimize the penetrating of blood and thus benefit in the interfacial bonding between the coatings and substrate during degradation. Previous investigations confirmed that PTMC could significantly decrease the corrosion of magnesium substrates owing to the surface erosion behavior [18]. When combined with a sulfobetaine bearing polymer PSB, a hybrid polymer layer (PTMC–NHCO–PSB) inhibited platelet deposition and adhesion of smooth muscle cell [19]. Yuan et al. [20] revealed that a Mg alloy esophageal stent with PCL-PTMC coatings exhibited no signs of cell toxicity to the epithelial and smooth muscle cell layers when used *in vivo*. Therefore, it is expected that PTMC, which exhibits surface erosion behavior with neutral degradation product, would slow down the corrosion of magnesium substrate and show good cytocompatibility.

Herein, we report the fabrication of PTMC coatings with surface erosion behavior to improve the corrosion of magnesium substrate. Fluoride and subsequent silane pretreatment was developed to improve the corrosion resistance of magnesium substrate and adhesion strength of polymer coating. PTMC coatings with different molecular weights were applied and the effect of polymer molecular weight on magnesium alloys in terms of degradation behavior, cyto- and hemocompatibility were systematically investigated. Furthermore, a conventional antiproliferative drug, paclitaxel, was incorporated into the PTMC coatings. The drug releasing behavior and the bioactivity of the releasate was evaluated by determining its effect on smooth muscle cells proliferation.

2. Experimental section

2.1. Materials and coating preparation

All the samples used in the present study were manufactured out of the as-extruded AZ31B magnesium alloy supplied by Jiaozuo Anxin Magnesium Alloys Scientific Technology Co., Ltd., China. Disc samples with dimensions of $10 \times 5 \times 1$ mm^3 were prepared for corrosion, blood contacting tests and cell experiments. All the samples were grounded with SiC papers up to 2000 grit and then ultrasonically cleaned in acetone, absolute ethanol and distilled water for 5 min each. The coating materials were PTMC with two different molecular weights of 50,000 g/mol (PTMC5) and 350,000 g/mol (PTMC35). PLGA (50:50 LA:GA) with an average molecular weight of 100,000 g/mol was used as control. Before the polymer coating procedure, the samples were pre-treated by 40% hydrofluoric acid for 72 h to allow the formation of fluoride layers [21]. The fluoridized substrates were subjected to the air plasma treatment for 5 min to clean and activate the surface. After that, the samples were immersed in 5% APTES solution [22], and then cured at 120 °C for 30 min. The polymeric coating was synthesized by mixing the polymers in dichloromethane, as a solvent, in concentrations of 1% (w/v). The viscosity in dichloromethane is 1.03 dl/g for PTMC5, 4.7 dl/g for PTMC35 and 0.67 dl/g for PLGA. PTMC and PLGA coatings were deposited on the substrates through simple dip-coating method [23]. After dipping for 30 s, the substrate was withdrawn at a constant speed and the dip coating process was repeated several times to obtain the thickness uniform coating. Then the coated samples were dried in vacuum. Prior to the cell experiments, all the samples were sterilized under ultraviolet radiation for at least 4 h.

2.2. Coating characterization

Coating morphologies were observed using an environmental scanning electron microscopy (ESEM, Quanta 250FEG, FEI). The samples were mounted in epoxy resin and cross-section morphologies and coating thickness were observed by SEM. The structure of polymer coatings was determined by Fourier transform infrared spectroscopy (FTIR) over a scan range of 3500 to 500 cm^{-1}. To determine the adhesion of polymer coatings on the substrates, the lap-shear test was conducted on an Instron 1195 machine according to ISO 4587:2003. A pair of samples ($60 \times 10 \times 2$ mm^3) was stacked with an overlapped area of 20×10 mm^2 and glued with Loctite 401. The samples were then pulled in opposite directions at a speed of 1 mm/min until their detachment. Measurements were repeated three times for each sample at room temperature.

2.3. Corrosion tests

Electrochemical and immersion measurements were performed in terms of ASTM-G31-72 in Hank's solution (NaCl 8.0g, KCl 0.4g, $CaCl_2$ 0.14g, $NaHCO_3$ 0.35g, Glucose 1.0g, $MgCl_2{\cdot}6H_2O$ 0.1g, $MgSO_4{\cdot}7H_2O$ 0.06g, $Na_2HPO_4{\cdot}12H_2O$ 0.06g, K_2HPO_4 0.06g dissolve in 1 L ultrapure water) at 37 °C.

Electrochemical tests were carried out by an electrochemical workstation (CHI660, Chenhua) with three-electrode system. The saturated calomel electrode (SCE) was reference electrode, a platinum electrode and the experimental samples served as the counter electrode and working electrode, respectively. The exposed area of the working electrode to the electrolyte was 1.0 cm^2. Potentiodynamic polarization curves were recorded with a scan rate of 1 mV/s from −1.9 to −1.0 V after the stabilization of open circuit potential for 30 min.

Immersion tests were used to characterize the static corrosion behavior. The hydrogen evolution volume was measured as a function of the immersion time. After different immersion intervals, samples were removed from the solution, gently rinsed with distilled water and dried at room temperature. The changes of surface morphologies were characterized by ESEM. The magnesium ion releasing was measured by inductively coupled plasma atomic emission spectrometry (Profile ICP-AES, Leeman Labs). An average of three measurements was taken for each group.

2.4. Surface erosion behavior

PTMC with average molecular weight of 350,000 g/mol was cast on the surface of magnesium substrate to obtain a thick polymer coating. Previous studies indicate that PTMC is susceptive to enzymolysis and exhibits faster degradation in the presence of lipase [24]. In order to make the phenomenon more obvious, the surface erosion behavior of PTMC coating was performed in lipase containing Hank's solution with a concentration at 500 U/L at 37 °C with gentle shaking. The lipase solutions were refreshed every 48 h. At different time intervals, the PTMC coated specimens were washed with distilled water and dried in vacuum. The cross-section morphologies and the coating thickness were observed by ESEM.

2.5. Drug releasing profile measurement

Paclitaxel loaded polymers were prepared by solubilizing paclitaxel (10 wt% to polymer) into the polymer/solvent mixture prior to the dip-coating procedure described in Section 2.1. The polymer coated samples were immersed in Hank's solution at 37 °C in the shaker. At different immersion periods, the releasate solution was collected and fresh Hank's solution was added. The paclitaxel in the collected releasate was detected at 230 nm using an ultraviolet spectrometer. Three separate samples were measured for each polymer type.

2.6. Hemocompatibility

The hemolysis test was carried out according to ISO 10993-4:2017 [25] and direct contact method was adopted. Fresh whole rabbit blood with 3.8% sodium citrate as anticoagulant was obtained and diluted with normal saline in a volume ratio of 5:4 (V_{saline}:V_{blood}). The samples were incubated in 10 ml normal saline at 37 °C for 30 min. Afterwards, 0.2 ml diluted blood was added and the mixtures were incubated at 37 °C for 60 min. Subsequently, blood mixtures were centrifuged at 3000 rpm for 5 min and the supernatant was carefully removed for spectroscopic analysis at 545 nm by an ultraviolet spectrophotometer (SmartSpec 3000, Bio-Rad Laboratories, Inc.). The control groups involved the normal saline as negative control and the distilled water as positive control. Three replicates were used for the hemolysis test. The hemolysis ratio is calculated via the following equation:

$$\text{Hemolysis ratio } (\%) = \frac{(A - C_1)}{(C_2 - C_1)} \times 100\%$$

Where A is the absorbance of the sample, C_1 is the absorbance of the negative control and C_2 is the absorbance of the positive control.

The blood was centrifuged at 1000 rpm for 20 min to obtain platelet-rich plasma (PRP). 150 μl PRP was added on the surface of samples and incubated at 37 °C for 1 h. The samples were rinsed three times with PBS, fixed in 2.5% glutaraldehyde for 1 h, and dehydrated using graded ethanol to 100%. The morphologies of platelet adhesion on samples were observed by ESEM.

2.7. Human vascular smooth muscle cell growth inhibition

Human umbilical vein vascular smooth muscle cells (HUVSMC) were cultured in Smooth Muscle Cell medium (SMCM, Sciencell), 10% fetal bovine serum (FBS), 100 U ml^{-1} penicillin and 100 μg ml^{-1} streptomycin at 37 °C in a humidified atmosphere of 5% CO_2. 5×10^4 cells with 1 ml SMCM were seeded and co-cultured with the samples in 24-well plates. The cell culture medium was exchanged every 2 days. After 2 and 5 days culture, the fresh culture medium containing 10% Cell Counting Kit-8 (CCK-8, Dojindo) was added to each well for 3 h in the incubator. The absorbance of the samples was measured by a microplate reader (Varioskan LUX, Thermo Scientific Inc.) at 450 nm. Additionally, the cell growth on the polymer coating was also evaluated by AO/BE double staining (Solarbio) and observed by a fluorescence microscope (Olympus, Japan).

2.8. Statistical analysis

The results are represented as mean ± standard deviation. Statistical analysis was conducted by one-way ANOVA, followed by Turkey's testing. The significance was defined as 0.05.

3. Results

3.1. Coating characterization

The surface and cross-sectional morphologies of the bare, HF treated and PTMC coated magnesium alloys are presented in Fig. 1. The bare substrates show clear scratches resulting from the mechanical polishing. After HF treatment and subsequent PTMC coating, the samples exhibit a flat surface with only slight scratch remnants. The cross-sectional morphology reveals an average coating thickness of ~5 μm (Fig. 1d). The HF-treated layer cannot be distinguished from the PTMC coating, which might be due to its low thickness ~100 nm [26]. FTIR spectrum (Fig. 1e) of the APTES-treated sample clearly shows peak around 1045 cm^{-1} that corresponds to Si-O asymmetric stretching in -*Si-O*-Si- [27,28] and peak around 755 cm^{-1} revealing the amine groups [29]. Subsequent PTMC coating significantly decreases the intensities of these peaks, with the appearance of peaks around 1745 cm^{-1} and 1230 cm^{-1} that are assigned to the characteristic peaks of PTMC, such as C=O and C-O stretching vibrations. It implies the existence of PTMC coating, which is consistent to the FTIR spectra in other published researches [28,30–33]. In Fig. 1f, the bonding strength between PTMC coating and substrate is compared with those obtained after plasma- and silane-treatment. A

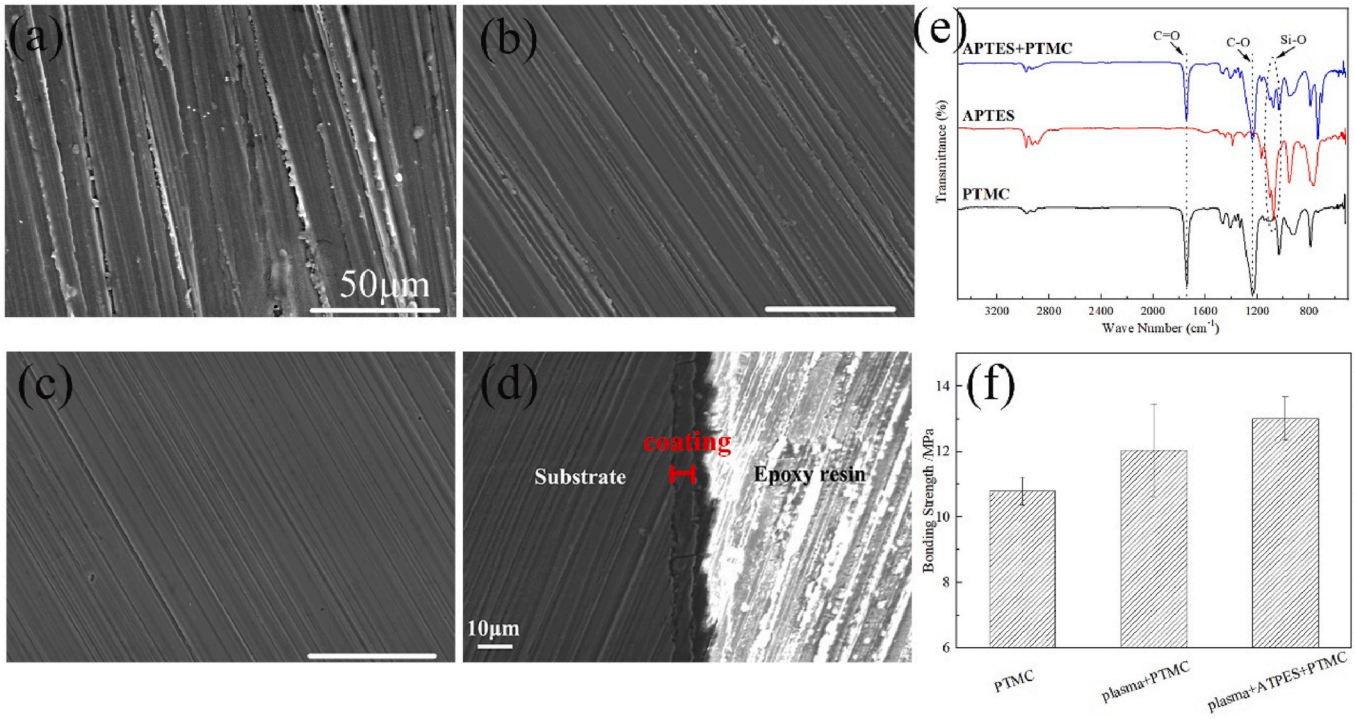

Fig. 1. Surface morphologies of (a) bare, (b) fluoride treated and (c) PTMC coated magnesium alloys and (d) the cross-sectional morphology of (c), (e) FTIR spectra and (f) the bonding strength of PTMC coatings.

21.5% improvement of the bonding strength is obtained for the samples with plasma and the subsequent silane treatment, respectively.

3.2. In vitro corrosion tests

Fig. 2 compares the potentiodynamic polarization (PDP) plots measured from the fluoridized, PTMC and PLGA coated samples. The fitting data including values of corrosion potential (E_{corr}) and corrosion current density (I_{corr}) is shown in the inset table in Fig. 2. It can be seen that PTMC5 and PLGA coating show little effect on the cathodic process, while PTMC35 coating significantly reduces the cathodic current by an order of magnitude. The anodic parts demonstrate a current plateau and then accelerate to high corrosion rate, indicating the breakdown of coatings. Once the coating fails, extremely high polarization current is shown for PLGA coated sample. Amongst three coatings, PTMC35 coated sample exhibits the lowest anodic polarization current, suggesting its better protective effect over the other two coatings. The corrosion current densities are calculated based on the Tafel extrapolation. The slowest corrosion rate occurs in the case of PTMC35 coated sample (0.05 μA/cm^2), while PLGA exhibits 1.6 times higher corrosion rate than PTMC35 sample.

Fig. 3 displays the continuous immersion behaviors of various samples in Hank's solution for up to 20 days. HF treated and PTMC5 coated samples exhibit comparable Mg^{2+} releasing concentration, hydrogen evolution and pH change during the entire corrosion period. It is not consistent with the PDP results shown in Fig. 2 and could be attributed to the continuously changing corrosive medium and the sample surface during the whole 20 d immersion period. Fig. 3d presents the corrosion morphologies at different time intervals. HF treated and PTMC5 coated samples show similar trend for the initiation and subsequent enlargement of corrosion pits. After immersion for 20 days, corrosion pits with a diameter of about 100 μm are formed on the sample surface. It suggests that PTMC5 coating cannot provide effective protective effect of the magnesium substrate against corrosion. For PLGA coated sample, the Mg^{2+} releasing and hydrogen evolution are comparable with other samples for 9 days (Fig. 3b). At day 10, more corrosion pits disperse on the PLGA coated samples compared to those on others. Thereafter, the corrosion is strikingly accelerated, evidenced by the abrupt increased hydrogen evolution, which suggests the breakdown of PLGA coating. The abrupt increase of pH is not found, that might be due to the neutralization of the alkaline corrosion product of magnesium substrate and the acidic degradation product generated from PLGA. After 20 d corrosion, large corrosion pits with the diameter over 300 μm are formed (Fig. 3d) and the collected volume of hydrogen is over 10 times higher than HF treated samples. In the case of PTMC35 coating, it provides sustained protection even after 20 days corrosion, evidenced by the much lower concentration of Mg^{2+} (Fig. 3a) and the maintenance of the coating integrity at day 20 (Fig. 3d).

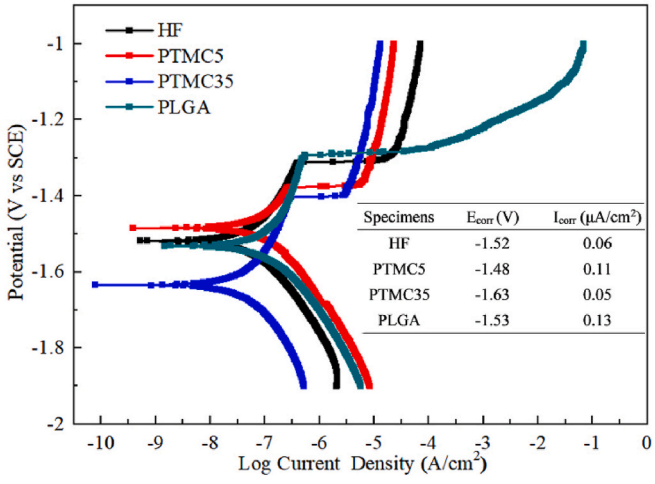

Fig. 2. Potentiodynamic polarization plots of PTMC and PLGA coated samples and the calculated electrochemical parameters are presented in the inset table.

3.3. Surface erosion of PTMC coating

The erosion of the PTMC coated samples at different time intervals is visualized by ESEM, as shown in Fig. 4. The surface of PTMC35 coating is smooth and compact, with a thickness of about 62 μm. As time extended, the PTMC35 coatings exhibit surface erosion behavior, as the outer surface of the coating becomes rougher and the coating thickness is uniformly thinned. No detachment of coating and the corrosion of magnesium substrate are observed as the coating erodes. The PTMC35 coatings indicate linearly reduction of coating thickness with prolonged immersion period. The PTMC coating degrades from exterior to interior and this erosion behavior can provide sustained protection of substrate against corrosion.

3.4. Drug release behavior

Fig. 5 plots the paclitaxel release profile of PTMC and PLGA coated samples. PTMC coated samples exhibit a two-phase release profile with a burst release of paclitaxel during the first 2 d. Thereafter, it shows a sustained and slower drug releasing, and the cumulative released percent is ~30% within 20 d. By contrast, there is nearly no paclitaxel release from the PLGA coated samples in the first 2 d. From 3 to 9 d, PLGA coated samples exhibits comparable drug release profile to PTMC samples and the amount of released paclitaxel reaches 16% at day 9. The abrupt accelerated drug release occurs afterwards and the cumulative drug release comes up to 60% after 20 d incubation.

3.5. Hemocompatibility

Fig. 6a presents the platelets assembled onto the surface of HF treated, PTMC and PLGA coated samples. With PLGA coating, an extremely large number of platelets is observed on the surface and most of them is activated to the extent of dendritic spreading state in the pseudo-podium stage. A small number of platelets is adhered on the HF treated samples and some are activated to dendritic spreading state. Although the number of adhered platelets on PTMC coatings exhibit no significant difference from those on HF group (Fig. 6b), it is noteworthy that platelets on the PTMC coating are still in a round state. Fig. 6c compares the hemolysis ratio of various samples and the PTMC and PLGA coated samples show the hemolysis ratio of 2.2–3.98%, which is acceptable for clinical requirements (<5%).

3.6. Human vascular smooth muscle cell growth inhibition

The bioactivity of released paclitaxel from PTMC and PLGA coated samples are evaluated by placing drug-loaded samples into cell culture wells preseeded with HUVSMCs. Without paclitaxel releasing, PTMC35 coated samples exhibit good cell viability at day 2 and 5, while only 50% cell viability is observed for PLGA group (Fig. 7a). When the PTMC35 coatings containing paclitaxel are present in the culture wells, HUVSMCs viability is significantly reduced. However, no significant reduction in cell viability is observed for PLGA-PTX samples. HUVSMCs were also seeded onto the samples to determine the antiproliferative activity of paclitaxel released from coatings. It can be seen that, after 2 d, HUVSMCs are well adhered and exhibit elongated cell morphologies on PTMC and PLGA coatings. Without paclitaxel present, HUVSMCs exhibit substantial cell proliferation up to 5 d. Enhanced cell proliferation is observed on PTMC coated magnesium alloy versus the PLGA coated one. The cell growth is not influenced by the formation of gas bubbles on the sample surface. When seeding on coatings containing paclitaxel, the number of adhered cells is significantly decreased on day 2 and it does

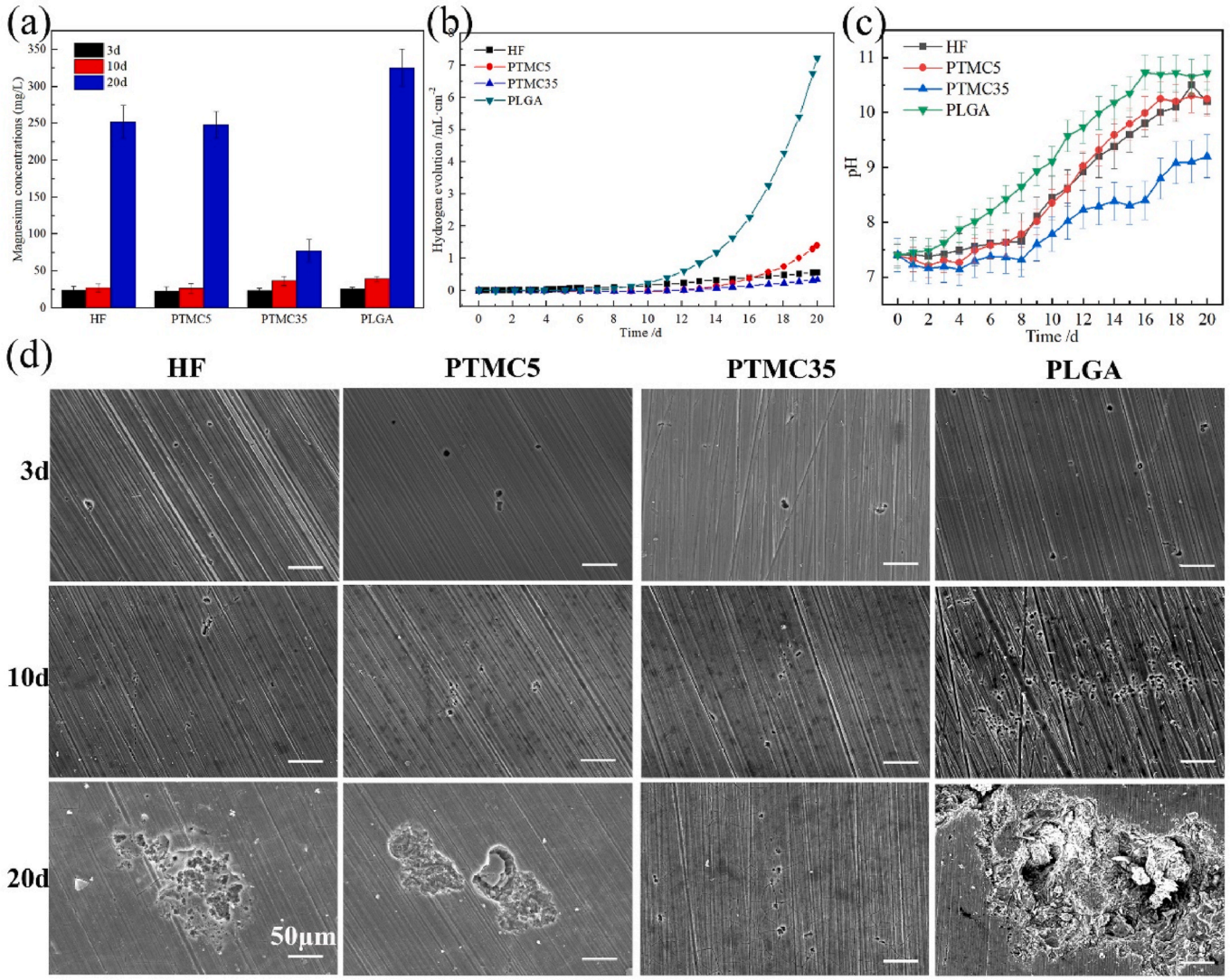

Fig. 3. In vitro corrosion measurements of PTMC and PLGA coated samples: (a) magnesium ion releasing, (b) hydrogen evolution behaviors, (c) pH change and (d) the corrosion morphologies.

not further increase until day 5 (Fig. 7b).

4. Discussion

Biodegradable polymer coatings are commonly applied for drug-eluting stent. However, polymer and metal have totally different physicochemical and mechanical properties, which results in relatively weak bonding at the interface. The coated polymer could be significantly deformed during the stent deployment and might cause the rupture or delamination of coating. The detached coating pieces would disturb the blood flow in the vessel and can be the source of acute vessel malfunctions [17]. In addition, the poor adhesion to the metal substrate also weakens the protective performance of coating [34] and results in hydrogen formation at the interface between magnesium and coating, which in turn aggravates the coating peeling-off. In this regard, the interfacial adhesion between polymer and magnesium should be firmly secured and fully evaluated.

In the present study, a sequence of pretreatment has been adopted to improve the adhesive bonding between polymer coating and magnesium substrate. The surface of magnesium alloys has been first modified by fluoride treatment to promote the formation of a $Mg(OH)_xF_{2-x}$ layer [35]. It can increase the corrosion resistance of magnesium substrate and can be used as a pretreatment process to improve the adhesion of PLA [36,37], PCL [38,39] and PEI [40] on magnesium substrate. After that, the fluoride surface has been modified via the introduction of amine groups through a combination of plasma and silane treatment. Plasma treatment easily generates many reactive species in the form of hydroxyl, peroxy, and carboxyl groups on the surface, which are active sites for the following chemical reactions and effectively increase the bonding strength between two substrates [41,42]. Mandofino et al. [43] indicated that when compared to the acetone cleaning, plasma treatment increased the joint strength on aluminum by 1.75 fold. Subsequently, a cross-linked silane layer is fabricated through the in situ APTES polycondensation and adhered to the substrate through silicon-oxygen bond. This solid polysilozane networks accompanied by the exposed amine functional group (Fig. 1e) would provide increased corrosion resistance of the substrate and improve the adhesive strength of the following polymer coatings by forming hydrogen bonding [44,45]. Liu et al. [22] introduced crosslinked APTES silane barrier on the surface of Mg-Zn-Y-Nd alloy before PLGA coating and the APTES pretreatment significantly increased the scratch resistance. With the introduction of the combined pretreatment, the bonding strength between PTMC coating and the substrate is increased by 21.5% due to the formation of chemical bonding and the hybrid adhesive layer [42].

PTMC coatings were prepared through simple dip-coating method in present study. This method is usually used to fabricate functional layers

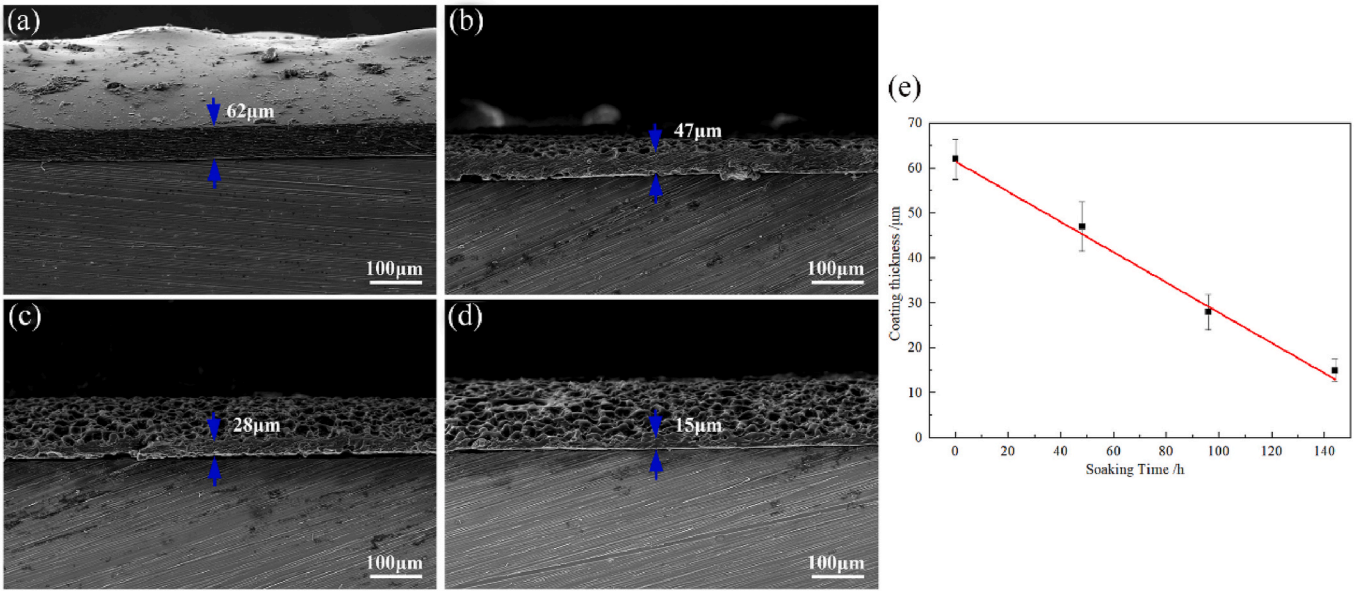

Fig. 4. The surface erosion of PTMC coating: cross-sectional morphologies of PTMC35 coated samples after (a) 0 h, (b) 48 h, (c) 96 h, and (d) 144 h corrosion and (e) the change of coating thickness as a function of immersion time.

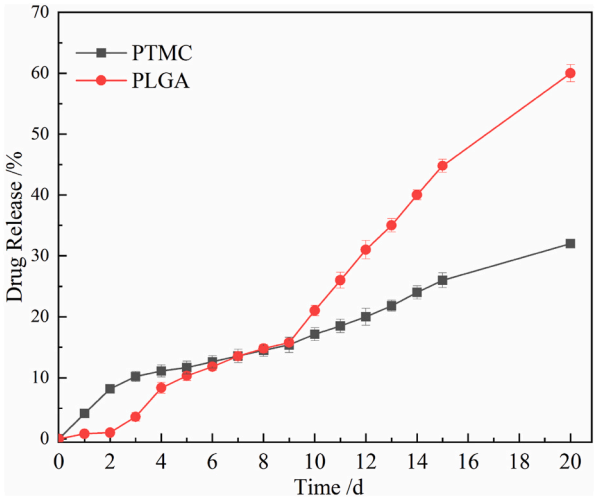

Fig. 5. Drug release profiles of PTMC and PLGA coated samples with paclitaxel.

and has been extensively utilized for research purposes owing to it being a convenient and facile approach. Coatings with the thickness of a few microns to hundreds of microns can be produced [46] and the coating thickness can be adjusted by modifying the viscosity of solution, the number of dipping cycles and draw-up speed from solution [47]. Dip-coating is also applicable for irregular and complex geometry like stent structure [48,49]. Guo et al. [50] prepared a PDLLA coating on magnesium alloy stent and the coating thickness can be controlled by the number of dipping cycles. A silica xerogel-chitosan hybrid coating was applied on the Co-Cr stent by dip-coating method and the coating exhibited a uniform distribution on all parts of the stents [51]. More importantly, the low glass transition temperature Tg (about −16 °C [52]) imparts good elastomeric mechanical properties to the PTMC coating. The elastomeric coating could better withstand the force exerted by the stent expansion procedure [53].

The degradation mode and degradation product of polymer coating has an important influence on the corrosion of magnesium alloy substrate and the associated drug releasing profile. Fig. 8 presents a schematic illustration of the corrosion of PLGA and PTMC coated magnesium alloys and the resulted drug releasing behavior. The slower observed initial PTX release from the PLGA coatings was observed during the first 2 d (Fig. 5) and was attributed to its higher Tg (>37 °C [54]). Therefore, the molecular motion and free volume of the amorphous polymer were limited, thus in turn inhibiting the PTX release from the bulk polymer. Similar phenomena is also reported in the literature of Gu et al. [54]. However, micropores and cracks can be easily formed in the PLGA coatings (Fig. 3d) owing to its self-accelerated bulk degradation mechanism [22,32]. The micropores or cracks permit the penetration or diffusion of aqueous solution which favors the water uptake and hydrolysis of both exterior and interior of PLGA coating. The acidic degradation product (i.e. lactic acid) from PLGA hydrolysis could react with magnesium substrate with the generation of alkaline corrosion products, such as hydrogen and $Mg(OH)_2$, precipitated at the interface [55]. The resulted local alkaline environment can also accelerate the coating degradation. At this stage, the drug release no longer depends on the diffusion control of the polymer but their degradation [56] and a rapid drug release profile is thus observed for PLGA coated samples during 3–9 d. In addition, the degradation of PLGA is further accelerated by the internal autocatalysis and induces the overall collapse of the polymer structure [22,32]. The protective effect of the coating is, therefore, largely destroyed, which abruptly speeds the magnesium corrosion kinetics after 9 d (Fig. 3b) and leads to the severe localized corrosion at day 20 (Fig. 3d). It was in accordance with Li's work, which reported a sudden accelerated corrosion of Mg-Zn after the breakdown of PLGA coating [57]. The solution pH value is increased to 9–11 (Fig. 3c), which can also catalyze the degradation of PLGA coating and hence further accelerated drug releasing rate is revealed during 9–20 d (Fig. 5).

In the case of PTMC coating, the sudden drug release occurs during 0–3 d, which may be due to the PTX molecules release from the coating surface. More importantly, PTMC exhibits a surface erosion behavior. The cleavage of their backbone is faster than water diffusion [18]. Thus the hydrolysis mainly occurs on the coating surface while the interior of coatings undergoes slight or no hydrolysis [32,58]. As a result, the PTMC coating is uniformly and gradually thinned in Hank's solution with the non-degraded coatings maintain intact structure and provide relative long-term protective effect to the substrate (Fig. 8). In addition, the neutral degradation product is friendly to magnesium alloy and may not accelerate the overall corrosion of magnesium substrate. With surface

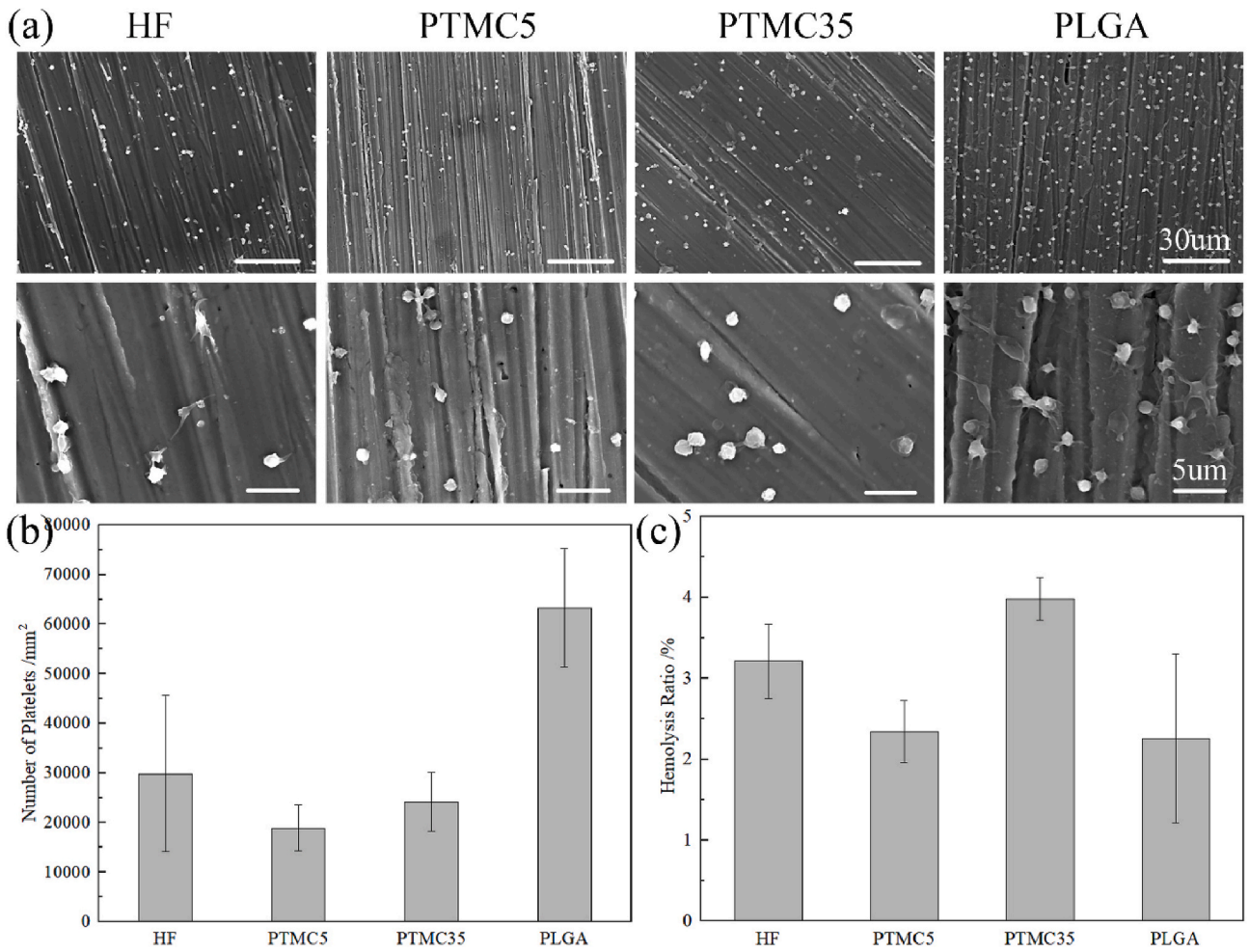

Fig. 6. (a) Representative morphologies of adherent platelets on the surface of PTMC and PLGA coated samples, (b) the number of platelets assembled on different coating surfaces and (c) hemolysis percentage.

erosion behavior and much slower degradation, PTMC coated samples show sustained paclitaxel released (Fig. 5). Only minor corrosion is hence occurred on PTMC coated magnesium substrate during the entire corrosion period (Fig. 3d). It was reported that the degradation rates of PTMC polymers increased with increasing molecular weight [24,59]. Surprisingly, the high molecular weight PTMC35 coating provides better protective effect for the magnesium substrate over low molecular weight PTMC5 counterparts in the present study. This observation may be related to the poor form-stability of low molecular weight PTMC [60]. Low molecular weight PTMC usually suffers serious deformation during degradation. This behavior may undermine the coverage and the associated protective effect of coating. Even though PTMC5 should exhibit much slower degradation rate than PTMC35, it is difficult to maintain the as-prepared or initial configuration and thus cannot provide sustained protection to Mg substrate.

The hemocompatibility of PTMC and PLGA coating was evaluated by hemolysis rate and platelet adhesion. In our study, the hemolysis rate of PTMC coated samples was below 5%, meeting the clinical requirements [2]. After the stent is implanted, the platelets will adhere to the endothelium, and if activated at the injury site, it will trigger the recruitment of more platelets to form a thrombus [61]. Unlike the PLGA coated and HF treated specimens, platelets attached to the PTMC coating remain round and inactive, possibly attributed to the protective effect of PTMC against substrate corrosion. It has been reported that hydrogen released by magnesium during incubation may lead to excessive platelet adhesion because localized hydrogen nuclei interfere with proteins in direct contact with platelets [62]. Both PTMC5 and PTMC35 coating samples have satisfactory results in terms of platelet morphology, adhesion amount and hemolysis rate. Vascular restenosis is an adverse phenomenon caused by tissue inflammation and excessive proliferation of smooth muscle cells after stent implantation, which is also one of the main concerns of stent implantation [63]. Inhibition of smooth muscle cell proliferation is thought to reduce the incidence of restenosis [64,65]. Paclitaxel, as an effective anti-inflammatory and anti-proliferative drug, is widely used in the research of DES vascular stents [66] and is loaded in the polymer coating in present study. With surface erosion behavior, PTMC coated samples show sustained paclitaxel released and exhibits a long inhibitory effect on HUVSMC proliferation. The HUVSMC inhibition results demonstrates the paclitaxel maintains bioactivity after polymer loading and solvent contact, suggesting feasibility for future application.

In summary, we have successfully prepared PTMC coatings with surface erosion behavior on magnesium substrate. When compared with PLGA coating, PTMC35 coating can significantly improve the corrosion resistance of magnesium substrate and exhibit sustained drug releasing profile during long-term corrosion period. PTMC coatings also reveal good hemo- and cyto-compatibility, showing great potential as a drug carrier material for stent applications.

Some notable limitations of the study should be mentioned here. First, the focus of this study was on preparing a surface eroded polymer layer and investigating its feasibility as a drug-eluting coating on magnesium alloy. The magnesium substrate used here is a commercial AZ31B alloy. The neurotoxic issue of the alloying element aluminum should pay close attention. Second, the flow of blood plays a key role on

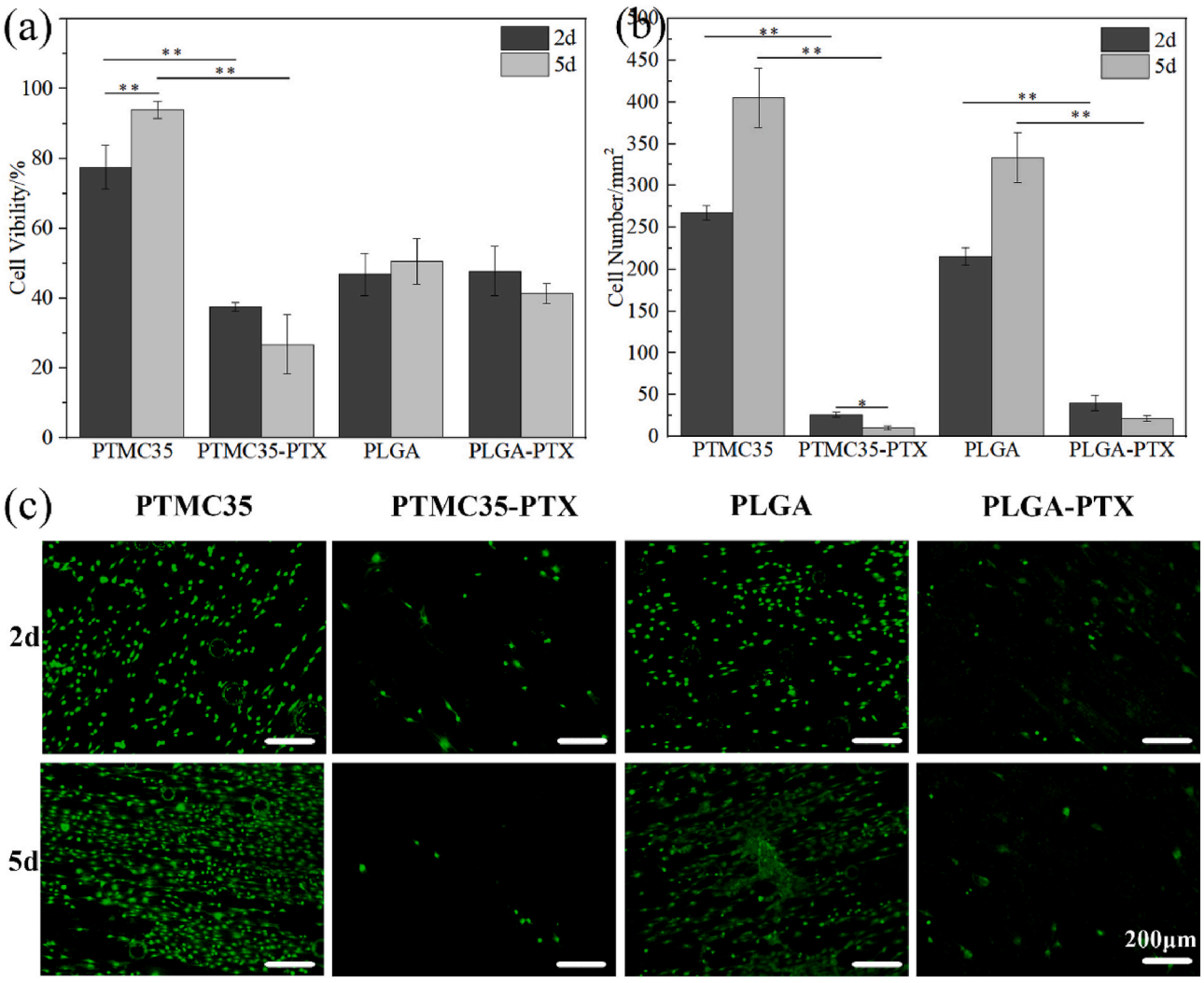

Fig. 7. (a) Cell viability, (b) quantitative analysis and (c) morphologies of HAVSMCs on the surface of PTMC and PLGA coated samples with or without paclitaxel. *P < 0.05 and **P < 0.01.

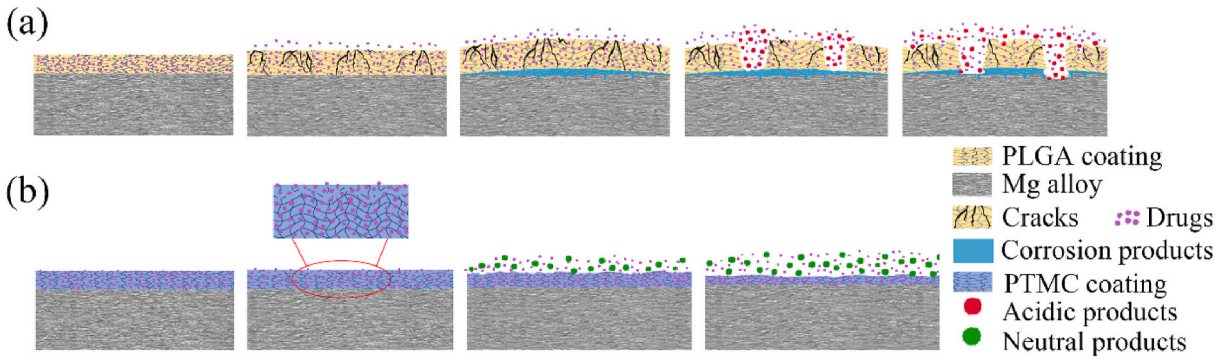

Fig. 8. Schematic illustration of the erosion models and drug release for (a) PLGA coated and (b) PTMC coated samples.

the initial stage of stent corrosion. The dynamic corrosion of PTMC coated samples should be evaluated, and the surface erosion behavior and associated drug release profile may be significantly affected by the flow induced shear stress. Further study could consider a systematic investigation into the surface erosion of coating, corrosion of substrate and drug releasing of PTMC coated magnesium when the flow is applied on the sample.

5. Conclusion

In this study, we developed the PTMC coating with different molecular weight on magnesium alloys and investigated its feasibility as drug-eluting coatings for stent applications. The in vitro corrosion behavior, drug release profile and the biocompatibility of PTMC coated samples were evaluated, taking PLGA coated ones as control. The following conclusions can be drawn:

1. PTMC coating exhibited surface erosion behavior and high molecular weight PTMC35 coating provided long-lasting protection for the substrate with only scattered corrosion pits observed after 20 d corrosion. The corrosion rate of PTMC35 coated samples exhibited much slower corrosion rates 0.05 μA/cm^2 than the low molecular weight PTMC counterparts (0.11 μA/cm^2) and the PLGA control (0.13 μA/cm^2).
2. PTMC coating indicated more stable and sustained paclitaxel release than the PLGA coating, which effectively inhibited the HUVSMC proliferation. The cumulative drug release came up to 30% after 20 d incubation.
3. PTMC coated samples showed good cyto- and hemo-compatibility with only few platelets adhered on them. The hemolysis ratio of PTMC coated sample is 3.98% which is satisfactory for clinical requirements (<5%).

CRediT authorship contribution statement

Hongyan Tang: designed and performed research, analyzed data, wrote the paper. **Shuangshuang Li:** designed and performed research. **Yuan Zhao:** analyzed data. **Cunli Liu:** analyzed data. **Xuenan Gu:** designed and performed research, wrote the paper, supervised research. **Yubo Fan:** supervised research.

Declaration of competing interest

The authors declare that they have no conflicts of interest to this work.

Acknowledgement

This work was supported by the National Key R&D Program of China (2018YFC1106600), the National Natural Science Foundation of China (52071008, 11827803), Beijing Natural Science Foundation (2192027), Young Elite Scientists Sponsorship Program By CAST (2017QNRC001).

References

[1] M. Haude, H. Ince, A. Abizaid, R. Toelg, P.A. Lemos, C. von Birgelen, E. H. Christiansen, W. Wijns, F.J. Neumann, C. Kaiser, E. Eeckhout, S.T. Lim, J. Escaned, H.M. Garcia Garcia, R. Waksman, Safety and performance of the second-generation drug-eluting absorbable metal scaffold in patients with de-novo coronary artery lesions (BIOSOLVE-II): 6 month results of a prospective, multicentre, non-randomised, first-in-man trial, Lancet 387 (10013) (2016) 31–39.
[2] Y.X. Yang, Z. Fang, Y.H. Liu, Y.C. Hou, L.G. Wang, Y.F. Zhou, S.J. Zhu, R.C. Zeng, Y.F. Zheng, S.K. Guan, Biodegradation, hemocompatibility and covalent bonding mechanism of electrografting polyethylacrylate coating on Mg alloy for cardiovascular stent, J. Mater. Sci. Technol. 46 (2020) 114–126.
[3] X.N. Gu, Y.F. Zheng, A review on magnesium alloys as biodegradable materials, Front. Mater. Sci. China 4 (2010) 111–115.
[4] X.N. Gu, N. Li Barr, W.R. Zhou, Y.F. Zheng, X. Zhao, Q.Z. Cai, L.Q. Ruan, Corrosion resistance and surface biocompatibility of a microarc oxidation coating on a Mg-Ca alloy, Acta Biomater. 7 (2010) 1880–1889.
[5] X.N. Gu, X.H. Xie, N. Li, Y.F. Zheng, L. Qin, In vitro and in vivo studies on a Mg–Sr binary alloy system developed as a new kind of biodegradable metal, Acta Biomater. 8 (6) (2012) 2360–2374.
[6] R. Waksman, R. Erbel, C. Di Mario, J. Bartunek, B. de Bruyne, F.R. Eberli, P. Erne, M. Haude, M. Horrigan, C. Ilsley, D. Böse, H. Bonnier, J. Koolen, T.F. Lüscher, N. J. Weissman, Early and long term intravascular ultrasound and angiographic findings after bioabsorbable magnesium stent implantation in human coronary arteries, JACC Cardiovasc. Interv. 2 (4) (2009) 312–320.
[7] R.C. Zeng, L.Y. Cui, K. Jiang, R. Liu, B.D. Zhao, Y.F. Zheng, In vitro corrosion and cytocompatibility of a microarc oxidation coating and poly(L-lactic acid) composite coating on Mg-1Li-1Ca alloy for orthopedic implants, ACS Appl. Mater. Interfaces 8 (15) (2016) 10014–10028.
[8] D.B. Panemangalore, R. Shabadi, M. Gupta, G. Ji, Effect of fluoride coatings on the corrosion behavior of Mg–Zn–Er alloys, Surf. Interfaces 14 (2019) 72–81.
[9] R.M. Lozano, B. Pérez Maceda, M. Carboneras, E. Onofre Bustamante, M.C. Garcia Alonso, M. Escudero, Response of MC3T3-E1 osteoblasts, L929 fibroblasts, and J774 macrophages to fluoride surface-modified AZ31 magnesium alloy, J. Biomed. Mater. Res. 101 (10) (2013) 2753–2762.
[10] H. Yang, K. Xia, T. Wang, J. Niu, Y. Song, Z. Xiong, K. Zheng, S. Wei, W. Lu, Growth, in vitro biodegradation and cytocompatibility properties of nano-hydroxyapatite coatings on biodegradable magnesium alloys, J. Alloys Compd. 672 (2016) 366–373.
[11] P. Makkar, H.J. Kang, A.R. Padalhin, O. Faruq, B. Lee, In-vitro and in-vivo evaluation of strontium doped calcium phosphate coatings on biodegradable magnesium alloy for bone applications, Appl. Surf. Sci. 510 (30) (2020), 145333.
[12] W. Xu, K. Yagoshi, Y. Koga, M. Sasaki, T. Niidome, Optimized polymer coating for magnesium alloy-based bioresorbable scaffolds for long-lasting drug release and corrosion resistance, Colloids Surf. B Biointerfaces 163 (2018) 100–106.
[13] A. Witecka, A. Yamamoto, J. Idaszek, A. Chlanda, W. Święszkowski, Influence of biodegradable polymer coatings on corrosion, cytocompatibility and cell functionality of Mg-2.0Zn-0.98Mn magnesium alloy, Colloids Surf. B Biointerfaces 144 (2016) 284–292.
[14] P. B, D.j. Guo, N. Nagiah, W. Tan, Evaluation of electrospun PLLA/PEGDMA polymer coatings for vascular stent material, J. Biomater. Sci. Polym. Ed. 27 (2016) 1–25.
[15] A. Strohbach, R. Busch, Polymers for cardiovascular stent coatings, Int. J. Poly. Sci. (2015), 782653.
[16] Y. Chen, Y. Song, S.X. Zhang, J.N. Li, C.L. Zhao, X.N. Zhang, Interaction between a high purity magnesium surface and PCL and PLA coatings during dynamic degradation, Biomed. Mater. 6 (2011), 025005.
[17] P. Sathyaraj, R. Kulandaivelu, S.N. Tsn, Improving the corrosion resistance and bioactivity of magnesium by a carbonate conversion-polycaprolactone duplex coating approach, New J. Chem. 44 (2020) 4772–4785.
[18] J. Wang, Y. He, M. Maitz, B. Collins, K. Xiong, L. Guo, Y. Yun, G. Wan, N. Huang, A surface-eroding poly(1,3-trimethylene carbonate) coating for fully biodegradable magnesium-based stent applications: toward better biofunction, biodegradation and biocompatibility, Acta Biomater. 9 (10) (2013) 8678–8689.
[19] Y. Chen, S.-H. Ye, Y. Zhu, X. Gu, S. Higuchi, G. Wan, W.R. Wagner, Covalently-attached, surface-eroding polymer coatings on magnesium alloys for corrosion control and temporally varying support of cell adhesion, Adv. Mater. Interfaces 7 (15) (2020), 2000356.
[20] T.W. Yuan, J. Yu, J. Cao, F. Gao, Y.Q. Zhu, Y.S. Cheng, W.G. Cui, Fabrication of a delaying biodegradable magnesium alloy-based esophageal stent via coating elastic polymer, Materials 9 (5) (2016) 384.
[21] L. Zhang, J. Pei, H. Wang, Y. Shi, J. Niu, F. Yuan, H. Huang, H. Zhang, G. Yuan, Facile preparation of poly(lactic acid)/brushite bilayer coating on biodegradable magnesium alloys with multiple functionalities for orthopedic application, ACS Appl. Mater. Interfaces 9 (11) (2017) 9437–9448.
[22] J. Liu, B. Zheng, P. Wang, X.G. Wang, B. Zhang, Q.P. Shi, T. Xi, M. Chen, S.K. Guan, Enhanced in vitro and in vivo performance of Mg–Zn–Y–Nd alloy achieved with APTES pretreatment for drug-eluting vascular stent application, ACS Appl. Mater. Interfaces 8 (28) (2016) 17842–17858.
[23] L.-Y. Li, L.-Y. Cui, R.-C. Zeng, S.-Q. Li, X.-B. Chen, Y. Zheng, M.B. Kannan, Advances in functionalized polymer coatings on biodegradable magnesium alloys – a review, Acta Biomater. 79 (2018) 23–36.
[24] Z. Zhang, R. Kuijer, S.K. Bulstra, D.W. Grijpma, J. Feijen, The in vivo and in vitro degradation behavior of poly(trimethylene carbonate), Biomaterials 27 (9) (2006) 1741–1748.
[25] I. 10993, Biological Evaluation of Medical Devices, Part 4: Selection of Tests for Interactions with Blood, 2017.
[26] T.T. Yan, L.L. Tan, B.C. Zhang, K. Yang, Fluoride conversion coating on biodegradable AZ31B magnesium alloy, J. Mater. Sci. Technol. 30 (7) (2014) 666–674.
[27] X. Liu, Z.L. Yue, T. Romeo, J. Weber, T. Scheuermann, S. Moulton, G. Wallace, Biofunctionalized anti-corrosive silane coatings for magnesium alloys, Acta Biomater. 9 (10) (2013) 8671–8677.
[28] J. Liu, B. Zheng, P. Wang, X.G. Wang, B. Zhang, Q.P. Shi, T.F. Xi, M. Chen, S. K. Guan, Enhanced in vitro and in vivo performance of Mg–Zn–Y–Nd alloy achieved with APTES pretreatment for drug-eluting vascular stent application, ACS Appl. Mater. Interfaces 8 (28) (2016) 17842–17858.
[29] S. Pourhashem, M.R. Vaezi, A. Rashidi, M.R. Bagherzadeh, Distinctive roles of silane coupling agents on the corrosion inhibition performance of graphene oxide in epoxy coatings, Prog. Org. Coating 111 (2017) 47–56.
[30] S. Sayyar, M. Bjorninen, S. Haimi, S. Miettinen, K. Gilmore, D. Grijpma, G. Wallace, UV cross-linkable graphene/poly(trimethylene carbonate) composites for 3D printing of electrically conductive scaffolds, ACS Appl. Mater. Interfaces 8 (46) (2016) 31916–31925.
[31] H. Yao, J.G. Li, N. Li, K.B. Wang, X. Li, J. Wang, Surface modification of cardiovascular stent material 316L SS with estradiol-loaded poly (trimethylene carbonate) film for better biocompatibility, Polymers 9 (2017) 598.
[32] K. Pan, X.J. Li, L. Meng, L. Hong, W. Wei, X.Y. Liu, Photo-cross-linked polycarbonate coating with surface-erosion behavior for corrosion resistance and cytocompatibility enhancement of magnesium alloy, ACS Appl. Bio Mater. 3 (7) (2020) 4427–4435.
[33] X.N. Gu, H.M. Guo, F. Wang, Y. Lu, W.T. Lin, J. Li, Y.F. Zheng, Y.B. Fan, Degradation, hemolysis, and cytotoxicity of silane coatings on biodegradable magnesium alloy, Mater. Lett. 193 (2017) 266–269.
[34] L.J. Zhang, E.A.A. Mohammed, A. Adriaens, Synthesis and electrochemical behavior of a magnesium fluoride-polydopamine-stearic acid composite coating on AZ31 magnesium alloy, Surf. Coating. Technol. 307 (2016) 56–64.
[35] T.F. da Conceicao, N. Scharnagl, C. Blawert, W. Dietzel, K.U. Kainer, Surface modification of magnesium alloy AZ31 by hydrofluoric acid treatment and its effect on the corrosion behaviour, Thin Solid Films 518 (18) (2010) 5209–5218.
[36] W. Ali, A. Mehboob, M.G. Han, S.H. Chang, Effect of fluoride coating on degradation behaviour of unidirectional Mg/PLA biodegradable composite for

load-bearing bone implant application, Compos. Appl. Sci. Manuf. 124 (2019), 105464.
[37] Z.L. Wang, Y. Guo, Corrosion resistance and adhesion of poly(L-lactic acid)/MgF2 composite coating on AZ31 magnesium alloy for biomedical application, Russ. J. Non-Ferrous Metals 57 (4) (2016) 381–388.
[38] P. Makkar, H.J. Kang, A.R. Padalhin, I. Park, B.G. Moon, B.T. Lee, Development and properties of duplex MgF2/PCL coatings on biodegradable magnesium alloy for biomedical applications, PloS One 13 (4) (2018), e0193927.
[39] J. Degner, F. Singer, L. Cordero, A.R. Boccaccini, S. Virtanen, Electrochemical investigations of magnesium in DMEM with biodegradable polycaprolactone coating as corrosion barrier, Appl. Surf. Sci. 282 (2013) 264–270.
[40] A. Zomorodian, M.P. Garcia, T. Moura e Silva, J.C.S. Fernandes, M.H. Fernandes, M.F. Montemor, Corrosion resistance of a composite polymeric coating applied on biodegradable AZ31 magnesium alloy, Acta Biomater. 9 (10) (2013) 8660–8670.
[41] L. Muñoz, F. Pineda, C. Martínez, M. Sancy, M. Urzua, M. Flores, M.V. Encinas, M. A. Páez, Improving the interaction between aluminum surfaces and polymer coatings, Surf. Coating. Technol. 358 (2019) 435–442.
[42] J. Choi, S.B. Cho, B.S. Lee, Y.K. Joung, K. Park, D.K. Han, Improvement of interfacial adhesion of biodegradable polymers coated on metal surface by nanocoupling, Langmuir 27 (23) (2011) 14232–14239.
[43] C. Mandolfino, E. Lertora, S. Genna, C. Leone, C. Gambaro, Effect of laser and plasma surface cleaning on mechanical properties of adhesive bonded joints, Procedia CIRP 33 (2015) 458–463.
[44] G.X. Tan, L. Zhang, C.Y. Ning, X.J. Liu, J.W. Liao, Preparation and characterization of APTES films on modification titanium by SAMs, Thin Solid Films 519 (15) (2011) 4997–5001.
[45] T.S.N.S. Narayanan, I.S. Park, M.H. Lee, 2 - surface modification of magnesium and its alloys for biomedical applications: opportunities and challenges, in: T.S.N. S. Narayanan, I.-S. Park, M.-H. Lee (Eds.), Surface Modification of Magnesium and its Alloys for Biomedical Applications, Woodhead Publishing, Oxford, 2015, pp. 29–87.
[46] A. Torabi, T.H. Etsell, P. Sarkar, Dip coating fabrication process for micro-tubular SOFCs, Solid State Ionics 192 (1) (2011) 372–375.
[47] I.A. Neacşu, A.I. Nicoară, O.R. Vasile, B.Ş. Vasile, Chapter 9 - inorganic micro- and nanostructured implants for tissue engineering, in: A.M. Grumezescu (Ed.), Nanobiomaterials in Hard Tissue Engineering, William Andrew Publishing2016, pp. 271-295.
[48] J.E. ten Elshof, 4 - chemical solution deposition techniques for epitaxial growth of complex oxides, in: G. Koster, M. Huijben, G. Rijnders (Eds.), Epitaxial Growth of Complex Metal Oxides, Woodhead Publishing2015, pp. 69-93.
[49] S. Ebnesajjad, A.H. Landrock, Chapter 8 - adhesive applications and bonding processes, in: S. Ebnesajjad, A.H. Landrock (Eds.), Adhesives Technology Handbook, third ed., William Andrew Publishing, Boston, 2015, pp. 206–234.
[50] L. Guo, L. Yu, Q. Zhao, X. Gong, H. Xie, G. Yuan, B. Li, X. Wan, Biodegradable JDBM coating stent has potential to be used in the treatment of benign biliary strictures, Biomed. Mater. 16 (2) (2021), 025010.
[51] T.-S. Jang, K.-H. Cheon, J.-H. Ahn, E.-H. Song, H.-E. Kim, H.-D. Jung, In-vitro blood and vascular compatibility of sirolimus-eluting organic/inorganic hybrid stent coatings, Colloids Surf. B Biointerfaces 179 (2019) 405–413.
[52] L.Q. Yang, B. He, S. Meng, J.Z. Zhang, M. Li, J. Guo, Y.M. Guan, J.X. Li, Z.W. Gu, Biodegradable cross-linked poly(trimethylene carbonate) networks for implant applications: synthesis and properties, Polymer 54 (11) (2013) 2668–2675.
[53] N. Abbasnezhad, N. Zirak, M. Shirinbayan, A. Tcharkhtchi, F. Bakir, On the importance of physical and mechanical properties of PLGA films during drug release, J. Drug Deliv. Sci. Technol. 63 (2021), 102446.
[54] X.Z. Gu, Z.W. Mao, S.H. Ye, Y. Koo, Y. Yun, T.R. Tiasha, V. Shanov, W.R. Wagner, Biodegradable, elastomeric coatings with controlled anti-proliferative agent release for magnesium-based cardiovascular stents, Colloids Surf. B Biointerfaces 144 (2016) 170–179.
[55] S. Agarwal, M. Morshed, M.N. Labour, D. Hoey, B. Duffy, J. Curtin, S. Jaiswal, Enhanced corrosion protection and biocompatibility of a PLGA–silane coating on AZ31 Mg alloy for orthopaedic applications, RSC Adv. 6 (115) (2016) 113871–113883.
[56] P. Lu, H.N. Fan, Y. Liu, L. Cao, X.F. Wu, X.H. Xu, Controllable biodegradability, drug release behavior and hemocompatibility of PTX-eluting magnesium stents, Colloids Surf. B Biointerfaces 83 (1) (2011) 23–28.
[57] J.N. Li, P. Cao, X.N. Zhang, S.X. Zhang, Y.H. He, In vitro degradation and cell attachment of a PLGA coated biodegradable Mg–6Zn based alloy, J. Mater. Sci. 45 (22) (2010) 6038–6045.
[58] M. Beck Broichsitter, Comparative in vitro degradation of surface-eroding poly (alkylene carbonate)s, Polym. Degrad. Stabil. 177 (2020), 109186.
[59] O.S. Kluin, H.C. van der Mei, H.J. Busscher, D. Neut, A surface-eroding antibiotic delivery system based on poly-(trimethylene carbonate), Biomaterials 30 (27) (2009) 4738–4742.
[60] L.Q. Yang, J.X. Li, W. Zhang, Y. Jin, J.Z. Zhang, Y. Liu, D.X. Yi, M. Li, J. Guo, Z. W. Gu, The degradation of poly(trimethylene carbonate) implants: the role of molecular weight and enzymes, Polym. Degrad. Stabil. 122 (2015) 77–87.
[61] R.X. Hou, L.G. Wu, J. Wang, N. Huang, Investigation on biological properties of tacrolimus-loaded poly(1,3-trimethylene carbonate) in vitro, Appl. Surf. Sci. 256 (16) (2010) 5000–5005.
[62] T. Hoshiba, M. Nikaido, M. Tanaka, Characterization of the attachment mechanisms of tissue-derived cell lines to blood-compatible polymers, Adv. Healthcare Mater. 3 (5) (2014) 775–784.
[63] Y.H. Fan, Y. Zhang, Q. Zhao, Y.H. Xie, R.F. Luo, P. Yang, Y.J. Weng, Immobilization of nano Cu-MOFs with polydopamine coating for adaptable gasotransmitter generation and copper ion delivery on cardiovascular stents, Biomaterials 204 (2019) 36–45.
[64] Y. Liu, Y.H. Wu, D. Bian, S. Gao, S. Leeflang, H. Guo, Y.F. Zheng, J. Zhou, Study on the Mg-Li-Zn ternary alloy system with improved mechanical properties, good degradation performance and different responses to cells, Acta Biomater. 62 (2017) 418–433.
[65] H.Y. Tang, F. Wang, D. Li, X.N. Gu, Y.B. Fan, Mechanical properties, degradation behaviors and biocompatibility of micro-alloyed Mg-Sr-RE alloys for stent applications, Mater. Lett. 264 (2020), 127285.
[66] Z.H. Wang, Q.X. Zheng, S.K. Guan, Z.B. Sun, S.P. Liu, B.B. Zhang, T.H. Duan, K. Xu, In vitro and in vivo assessment of the biocompatibility of an paclitaxel-eluting poly-l-lactide-coated Mg-Zn-Y-Nd alloy stent in the intestine, Mater. Sci. Eng. C 105 (2019), 110087.